A98-31537

ICAS-98-3,2,2

VORTICITY MEASUREMENTS IN THE NEAR-FIELD OF A WING TIP VORTEX

G. Lombardi, A. Talamelli,
Assistant Professor, Department of Aerospace Engineering, University of Pisa, Italy

J. Sjöberg
Master Student, Department of Mechanics, KTH, Stockholm, Sweden

Abstract

The initial phase of the roll-up of the wing tip vortex, emanating from high aspect ratio wings, is considered. An experimental investigation, based on hot-wire anemometry technique, is in progress; the measurement procedures used and some of the preliminary results are described. Tests are carried out on a tapered, no-swept wing model, with aspect ratio 5.7. The statistically averaged quantities of interest, viz. the three mean velocity components, the whole Reynolds stress tensor and the third order moments tensor, are measured, by combining different responses of the wires of single or X-wire probes positioned at different orientations in the measurement points. This procedure avoids the difficulties connected with the use and calibration of triple-wire probes and permits the use of considerably smaller and less intrusive probe. A continuous complex-wavelet transform technique is also used to assess some characteristics of the tip vortex wandering. Furthermore, to verify the results, a different measurement procedure, based on a pressure vorticimeter, has been used; it allows the time history of quantities related to the streamwise component of the vorticity to be obtained.

Introduction

The flow close to the wing tip is of the utmost relevance, not only for low aspect ratio wings, as, for instance, delta wings, but also for high aspect ratio wings. Indeed, the induced drag could be significantly affected by details of the spanwise lift distribution in that region; where an important introduction of energy in the field is concentrated. Furthermore, it is clear that upon increasing the wing span, the errors close to the wing tip, although small, could significantly affect the evaluation of the structural loads acting on the wing.[1]

The physical behavior of the fully developed tip vortex is well established. Starting from the pioneering work of Betz[2] and the more realistic description given by the model of Rankine and Lamb[3], several models were developed, such that of Rossow,[4] the viscous models of Hoffman and Joubert,[5] and Batchelor, [6] the turbulent model of Moore and Saffman[7]. Successively, different developments of these basic models were proposed, as, for instance, the modification of the Rankine-Lamb model presented by Staufenbiel,[8] and that of the Hoffman and Joubert model presented by Phillips.[9] Based on the above methods, numerical models correctly representing the fully developed tip vortex are available (see, e.g., the review presented by Hoeijmakers[10]). However, the initial roll-up of the wing tip vortex shows a more complex behavior than what can be deduced from the above models. In fact, the tip vortex evolves from a complex three-dimensional separated flow. The analysis carried out under the hypothesis of laminar flow (see for instance Moore and Saffman [7]) does not seem to be able to give a realistic representation of the initial roll-up process. Indeed, turbulence plays a primary role in the tip vortex formation process because of the complexity of the flow typology and the high Reynolds numbers usually involved.

In order to achieve a better understanding of the flow characteristics in the initial phase of the tip vortex roll-up, when emanating from high aspect ratio wings, an experimental investigation by means of hot-wire anemometry is in progress. In this paper the measurement procedures used and some of the preliminary results obtained are described.

Starting from the work of Chigier and Corsiglia[11] hot-wire probes have been extensively used for the analysis of this type of flow. Hot-wire techniques allow the full characterization of unsteady three-dimensional fields, but when the time-variations of the velocity components are requested, either the turbulence level is sufficiently low to allow some simplifications in the wire response equation, or resort must be made to a three or four wires probe. This may be a problem being the tip vortex susceptible to probe interference, [12] and using a 3-D hot wire probe its relevant dimension may be not sufficiently small to avoid such problems.

Many of the inconveniences encountered using hot-

wire anemometers, viz. high velocity gradients and interference effects, might be overcome using non intrusive techniques (see. Refs. [13], [14], [15] and [16]). However, in this case it must be checked that the particles, injected in the fluid, follow the flow satisfactorily. This might not be the case of tip vortex flows, which can be characterized by the presence of high rotational speed and strong centrifugal forces, which may deviate the particles trajectories.

Moreover, if all the statistically averaged quantities are of interest, viz. the three mean velocity components, the whole Reynolds stress tensor and the third order moments tensor, the use of non intrusive techniques may become more complicated, while hot-wire anemometry may provide easily reliable data despite its intrusivity and dimension. The measurement may be accomplished by combining different responses of the wires of single or X-wire probes positioned at different orientations in the measurement points. These procedures avoid the difficulties connected with the use and calibration of triple-wire probes and permit the use of considerably smaller and less intrusive probes.

Another aspect, which must be taken in to account, is the vortex wandering. In fact, many of the studies dealing with the tip vortex, especially those concerned with the characterization of the vortex well downstream, have encountered problems due to the unsteadiness of the flow, as demonstrated by Green and Acosta.[14] This implies that the core location at a specific downstream distance fluctuates erratically in time, and this meandering causes any time-averaged Eulerian point measurement to be actually a weighted average in both time and space[17]. It is thus evident that this unsteadiness of the flow may represent a significant problem for both numerical and experimental analysis. In the near field, up to one chord length downstream from the trailing edge tip, which is the region analyzed in the present investigation, the effects produced by this unsteadiness are usually not considered not significant.[16] To verify this assumption and to control the results given by the above described measurements procedure, a different technique, based on a vorticimeter[18] has been used, which allows the time history of quantities related to the streamwise component of the vorticity to be obtained.

Experimental set-up and measurements procedure

The experiments were carried out in the low-speed wind-tunnel of the University of Pisa. This is a closed return facility with a circular open test-section 1.1 m wide in diameter and 1.48 m long. The tunnel is equipped with a three-degree-of-freedom probe-transversing system capable of 0.1 mm minimum step sizes in the streamwise, spanwise and normal directions. Both data acquisition and traversing system are entirely automated and controlled by means of a PC. Flow-field measurements can be performed in a completely automatic process that allows the probe to be moved and oriented, performs the acquisition and the on-line temperature drift voltage error compensation as well as the preliminary data elaboration. The hot-wire probes are operated by a commercial anemometer system. Signal conditioner modules transform the bridge output voltages into a suitable range for an eight-channel simultaneous-sampling 16 bit A/D converter specifically designed for wind tunnel operations. In order to correct the anemometer output-voltages in case of ambient flow temperature variation, an on-line temperature correction procedure was implemented using high precision commercial integrated-circuit temperature sensors. Calibration of probes was carried out by performing a simultaneous velocity and angular sensitivity calibration as described in Ref. [19]. To calibrate the hot-wire probes a specific calibration unit along with computer-aided automated procedures and software were developed. Final data reduction is performed by means of Fortran programs.

Mean velocity components and the whole Reynolds stress tensor are evaluated by means of a digital processing of the signals acquired by X-wire probes at different orientations obtainable by rotating the probe around its axis.

In this method, developed for moderately three dimensional and relatively high turbulent flow,[20] the response equations for a hot-wire generically positioned in a moderately three-dimensional flow are used. The effective cooling velocity Q is assumed to be described with sufficient accuracy by the relation of Jorgensen,[21]

$$Q^2 = (V_n^2 + k^2 V_p^2 + h^2 V_{bn}^2) \qquad (1)$$

where V_n, V_p, and V_{bn} are the velocity components, respectively normal to the wire in the probe plane (defined by the directions of the wire and of the probe axis), parallel to the wire, and binormal to the previous ones; h and k are the direction sensitivity coefficients. These velocity components can be connected with those relative to the wind tunnel frame of reference v_x (streamwise), v_y (inboard), v_z (vertically upward) obtaining the following

$$Q^2 = A_1 v_x^2 + A_2 v_y^2 + A_3 v_z^2 + A_4 v_x v_y + A_5 v_x v_z + A_6 v_y v_z \qquad (2)$$

where the coefficients A_i are reported in Ref. [20]. Introducing the mean and fluctuating parts of the velocity components, and assuming a prevailing direction to exist (say U in direction x), eq. (2) may be expanded in binomial series. By retaining terms up to the third order in the ratio of the various components to U, we obtain a set of equations linking the mean and fluctuating effective velocity with the mean components and the second- and third-order moments of the velocity field.

Using a X-wire probe all the components of the mean

LOMBARDI

velocity and of the Reynolds stress tensor can be evaluated through digital processing of the signals successively acquired at four different orientations which can all be reached by positioning the probe in the direction of the prevailing component of the mean flow, and rotating it around its axis (Fig. 1). In this case, orientations, corresponding to the wire prongs being at high angles of attack, may be avoided reducing the interference problems, which are normally connected with the orientations of the conventional methods.

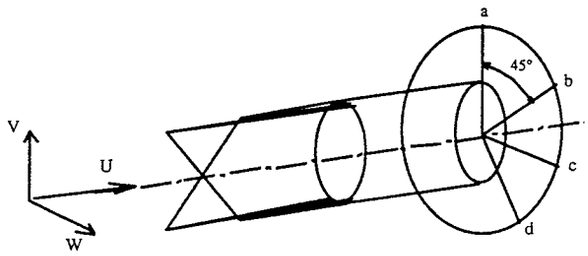

Fig. 1 - Positioning and rotational definition of the X-probe

The actual computation of the various components of the mean velocity vector and of the Reynolds stress tensor is obtained through an iterative procedure. In the first step approximations of the various quantities are obtained from the first part of the expressions described above, which are combinations of the mean or fluctuating effective velocities obtained at various wire orientations. In the successive steps of the iterations the second parts of the expressions, consisting of combinations of higher-order terms (including the triple correlation of the turbulence and third-order terms containing products of the y and z components of the mean velocity and of the second-order fluctuating terms) are evaluated using the values obtained in the previous step. The procedure normally converges in a few iterations, provided attention is paid to choose the acquisition lengths and the sampling rates in such a way that the various first-, second and third-order moments of the effective velocity are all sufficiently stationary, a fact that requires an appropriate preliminary analysis to be carried out. Thanks to a lower sensitivity to errors in probe calibration and positioning, the accuracy of this method was shown to be greater than that of previously available ones using similar probes. As all the methods using X-wire probes, this one is subject to errors produced by the existence in the flow of high gradients of the various quantities in the direction normal to the plane of the wires, which are usually separated by a distance of the order of 1 mm. For this reason the data-reduction software developed for this analysis has been provided with gradient error correction procedures implemented following Ref. [22].

The analyzed configuration

The wing model has zero twist and zero dihedral angle, aspect ratio 5.7, taper ratio 0.4, sweep angle, at 1/4 of the chord, $\Lambda=0°$ and a NACA 0012 wing section. A semi-model mounted on a horizontal plane is used. The analyzed configuration and the adopted geometric conventions are shown in Fig. 2. Experiments were conducted at a free-stream velocity of 18 m/s. The corresponding Reynolds number, based on the tip wing chord, is about $3x10^5$. In these preliminary analysis data have been obtained in a plane at one tip chord length from the wing trailing edge, at an angle of attack of 7.7 degree, corresponding to a lift coefficient of 0.612.[23]

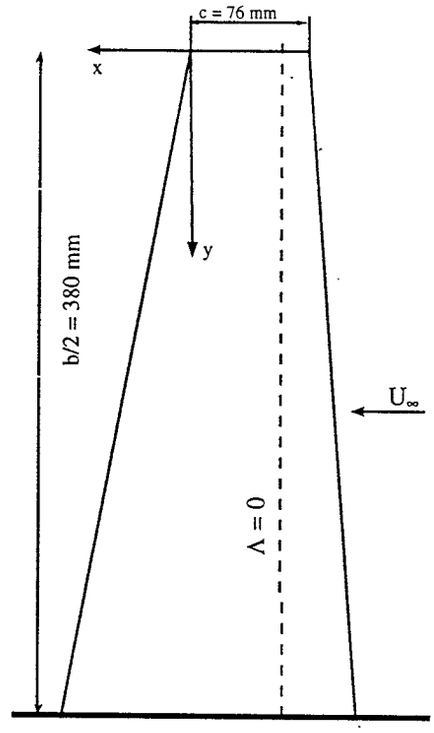

Fig. 2 - The analyzed configuration and the adopted conventions

The wing span is big enough to neglect the effects of the vortex image, due to the presence of the wall, and the interactions with the corner vortex at the root of the wing.

In this preliminary phase, data are obtained at a location of 1 chord length from the wing tip trailing edge. The size of the grid is 0.15 cm x 0.15 cm for a total number of 336 points[25].

Vortex characterization

The distribution of the longitudinal component of the normalized mean velocity flow-field (U/U_∞) is reported in Fig. 3. From this figure it may be noted the

LOMBARDI

presence of two distinct region: a wake where a clear discontinuity is present and a second region, close to the wing tip, characterized by a strong circulating and highly three-dimensional velocity field. The position of the wake is below the trailing edge, represented by a segment in the figure, due to the effects of the strong down-wash.

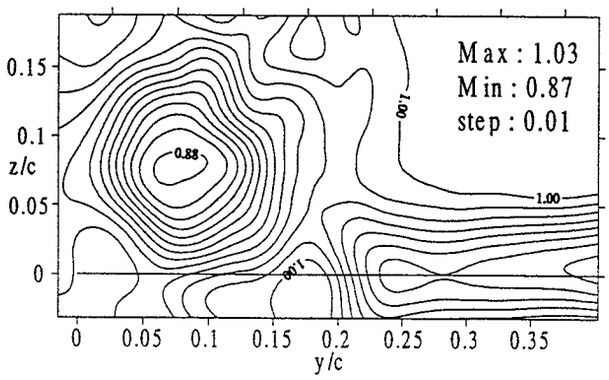

Fig. 3 – Iso-countours of the longitudinal component of the normalized mean velocity, U/U_∞

This effect is also depicted by the direction of the vectors close to the wake region, shown in Fig. 4. Behind the wing tip, the shear-layer coming from the wake is already rolled-up in an almost axisymmetric structure. From these

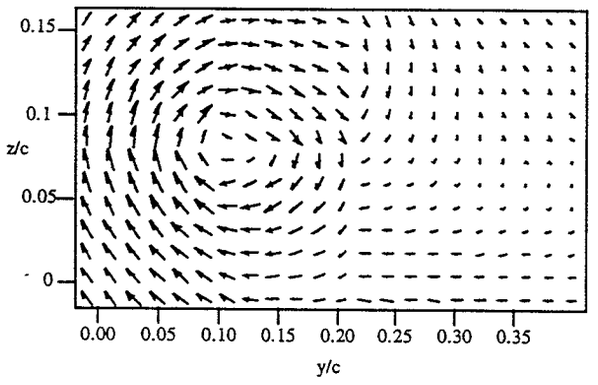

Fig. 4 - Velocity vectors in the wake region; plane normal to the freestream velocity.

measurements it is not possible to detect the presence of a spiraling structure of the vortex. The contour values show a decrease of the mean longitudinal component inside the vortex down to values of about 0.87 U_∞. While it is evident that the presence of a reduction inside the wake occurs, there is no obvious explanation to justify the same behavior inside the vortex region. The problem is still controversial and debated. For example Chow et al.[24] found that the high rotation produces low pressures in its core that accelerate incoming fluid to produce a large axial velocity surplus. However some authors showed an immediate formation of a deficit [15], while others found that the surplus persisted far downstream.[14]

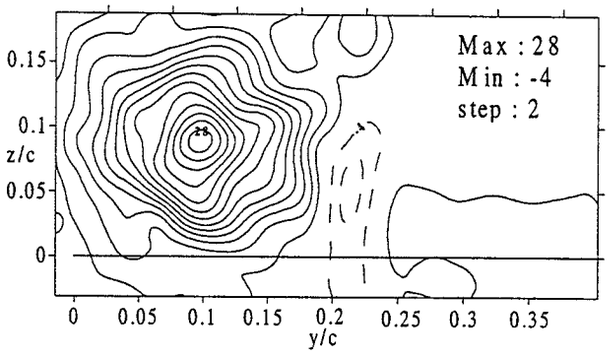

Fig. 5 – Iso-countours of the normalized longitudinal component of the mean vorticity, $\omega_x c/U_\infty$.

In Fig. 5 the contours of the normalized axial component of the mean vorticity are shown. These contours confirm that the vortex is already rolled-up in this position. The magnitude of the vorticity increases moving towards the core region. This peak is probably generated by the trapping of the vorticity coming from the wake, which contributes to increase its value. It is interesting the presence of a maximum of negative vorticity close to the border of the vortex. This may be due to the formation of a secondary structure induced by the main vortex.[1]

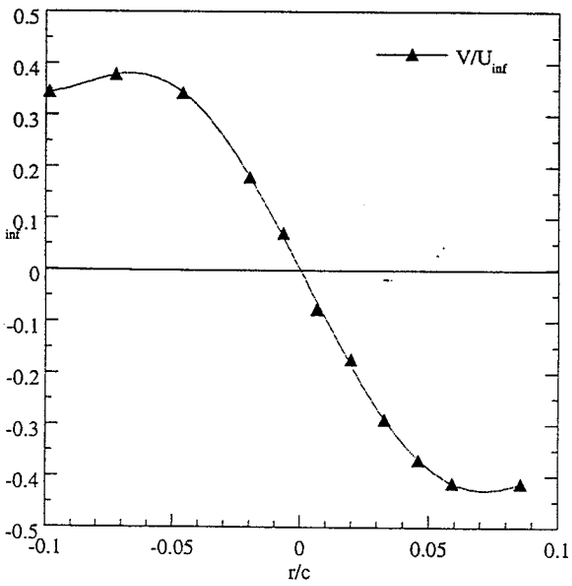

Fig. 6 - Section of the normalized tangential velocity, V/U_∞.

Dimension and characteristic of the vortex may be better assessed looking at Fig. 6, where the tangential velocity is reported. This figure shows the presence of two distinct regions. A vortex core where the velocity

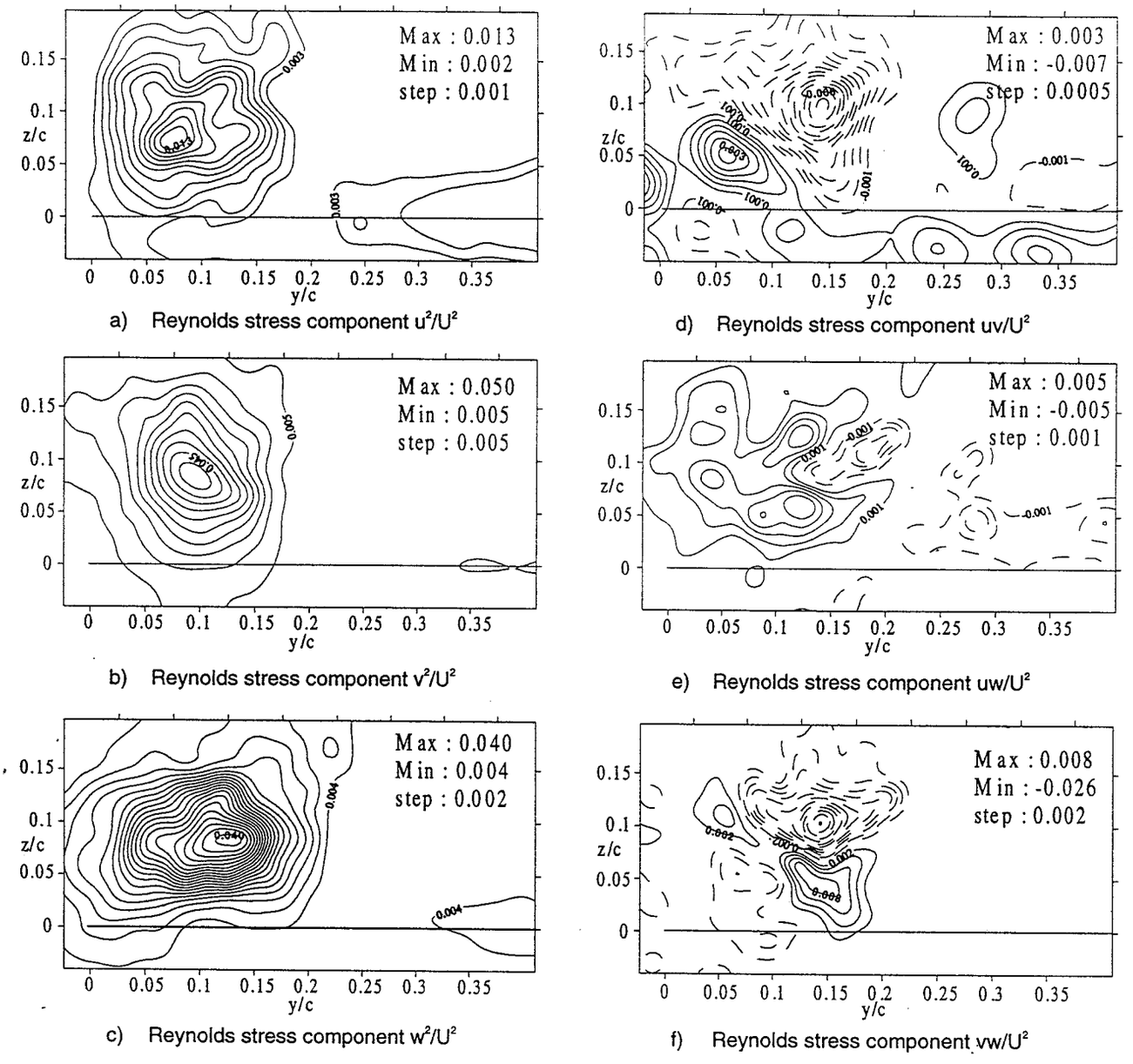

Fig. 7 – Iso-countours of the components of the Reynolds stress tensor.

growths linearly with the radius and an outer region where the velocity decreases with a hyperbolic law and the circulation is almost constant. However the grid is not fine enough to analyze the intermediate region where the velocity seems to follow different laws.[13] This figure permits also to estimate dimension and shape of the vortex, localizing the core where the transversal velocity becomes maximum, and to detect the position of the vortex-center.

Much information on the behavior of the turbulent flow-field in such a configuration may be obtained analyzing the components of the whole Reynolds stress-tensor (Fig. 7). Qualitatively, the spatial distributions of the turbulent kinetic energy q^2 (Fig. 8) resemble those corresponding to the mean streamwise vorticity component. The principal stresses of the Reynolds stress

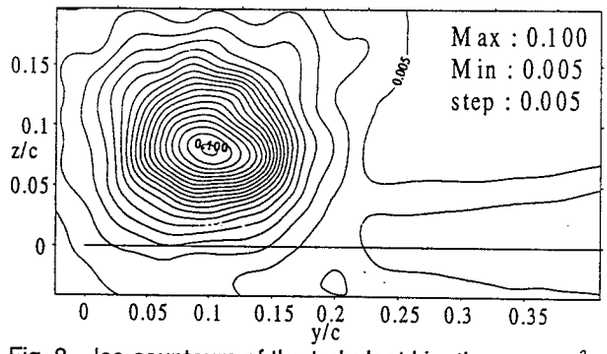

Fig. 8 – Iso-countours of the turbulent kinetic energy q^2.

LOMBARDI

tensor show a similar distribution, except in the vortex region where some differences appear. In particular the intensity of the streamwise component u^2 is weaker than the others. This is probably connected with the lower gradients of the mean axial velocity component. Moving downstream, this anisotropy of the Reynolds stress tensor decreases in connection with a more uniform distribution of the mean axial component in the measurement plane.
As far as the distribution of the mean turbulent kinetic energy is concerned, it may be observed that the maxima are located close to the vortex center. This behavior is in contrast with other results, which show a ring of high turbulence level surrounding the vortex core, and is more typical of split-wing vortices, which are formed by the merging of two tip-vortices.

Validation by means of a vorticimeter

In order to validate the results concerning the behavior of the mean axial vorticity component, obtained with this measurement procedure, a different measurement set has been accomplished by means of a different technique. For this purpose a new purpose-built pressure probe was used, which follows the theoretical concepts underlined in Ref. [18]. It is basically composed of four yaw-meters measuring the circulation around a circuit of 4 mm in diameter. This type of probe has the significant advantage of permitting a "direct" measurement of the circulation. The response of the instrument is a pressure difference, measured by means of a micro pressure transducer, mounted very close to the instrument. The adopted configuration allows the fluctuations of the streamwise vorticity component to be detected. The characteristics in terms of frequency response, calibration constant and accuracy of the instrument are reported in Ref. [18].

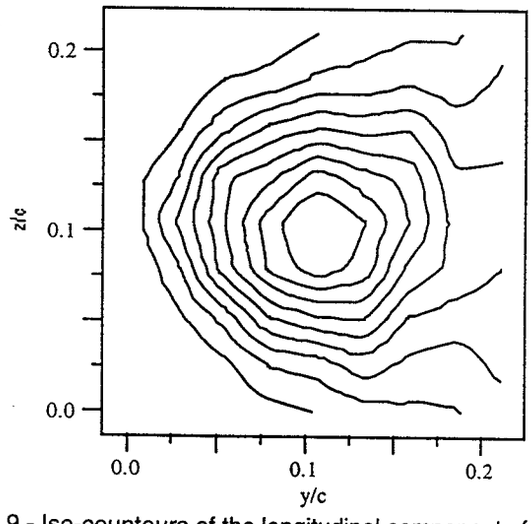

Fig. 9 - Iso-countours of the longitudinal component of the mean vorticity by the vorticity probe, normalized with the maximum value in the H-W measurements.
Min. value=0; Max value=0.96; step=0.12

In Fig. 9 the iso-countours of the mean axial vorticity, measured with this probe, are reported. This figure shows that position and vorticity distribution in the vortex are well depicted by the hot-wire technique. However, from these new measurements, the presence of a counter rotating secondary vortex, which was more evident in Fig.5, is not clear. Further increasing the dimension of the frame of the grid does not reveal any presence of such a vortex.

The problem of the vortex wandering

In Fig. 10 the r.m.s. values of the measurements carried out with the vorticimeter are shown.

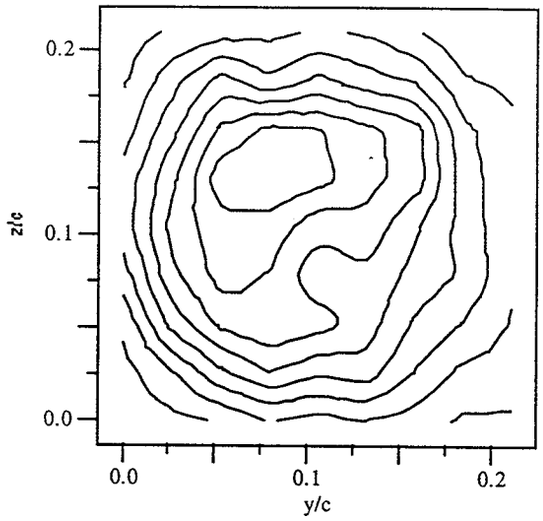

Fig. 10 - Iso-countours of the r.m.s. of the longitudinal component of the mean vorticity by the vorticity.
Min. value=0.02; Max value=0.16; step=0.02

The large fluctuations may indicate the presence of unsteadiness which may be not only associated with turbulent mixing. Hot-wire response offers interesting characteristics concerning this problem, the signals being continuous, low-noise and well suited to the measurements of velocity spectra. These techniques allow vortex wandering and other motions to be separated from turbulence phenomena. However, besides conventional Fourier analysis, processing procedures based on the continuous complex-wavelet transform have been also applied to the acquired velocity signals. The utility of this type of analysis in the present case stems from the intrinsic features of the wavelet transform, in which a signal is described by means of oscillating, zero mean, base function of compact support, i.e. whose values are zero or negligible outside a certain time interval, which defines the "scale" of the wavelet. By a process of convolution of the signal with dilated versions of these basic wavelets, the wavelet transform coefficients provide an evaluation of the "instantaneous" similarity of the signal with wavelets of different scale. By appropriately

LOMBARDI

connecting scales and inverse frequencies, it is thus possible to obtain the "instantaneous" contribution of the different frequencies to various physical quantities connected with the signal (e.g. its energy or its correlation with another signal). Obviously, this analysis is particularly suited when the fluctuations of a signal derive, rather than a sum of infinite sinusoidal waves, from the sum of finite "events", i.e. when the signal is intrinsically intermittent, as may indeed be considered the case for the phenomenon of wandering. In the literature several applications of the wavelet transform to the analysis of turbulent velocity signals are present [26], [27]; in these applications the wavelet transform are mainly used to enhance the flow field structures containing most of the turbulent energy, to evaluate their scales and to characterize their intermittent behavior. By means of the same mathematical tools it is possible to obtain power spectra, hereinafter wavelet spectra, which contain the same information of those obtained with Fourier transform. However, since it is possible, by means of this technique, to transform the velocity signal focusing the attention in a certain frequency range the wavelet spectrum results to be clearer and smoother than the Fourier one.

Indeed, in Fig. 11 the Fourier spectrum of a typical signal acquired does not show the presence of any particular periodic phenomenon except at very low frequencies where some peaks appear.

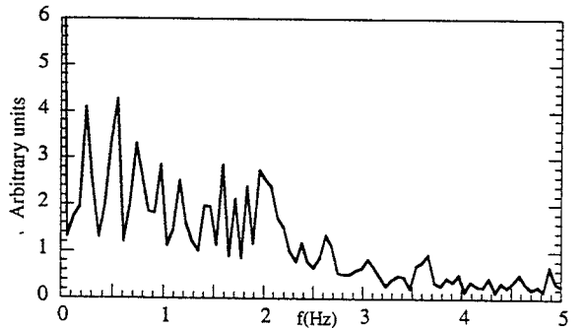

Fig. 11 - Fourier spectrum of the tangential velocity component.

Moreover, this classical analysis does not allow to estimate precisely the presence of certain prevailing frequencies even if the spectrum is obtained by averaging different spectra. In this case the error decreases despite the frequency resolution. On the contrary, the wavelet spectrum (Fig. 12), if focused in a specific low frequency range, shows a small hump at frequencies in the interval between 1.5 and 3 Hz. The wavelet technique has been applied to velocity signals acquired at 7-chord length from the tip trailing edge. At this distance the effect of the slow side-to-side movement of the vortex gives higher effects in the measured velocity signals.

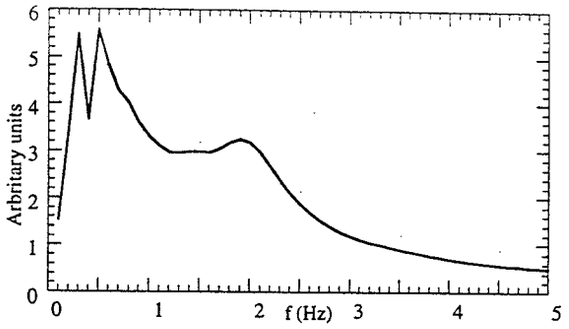

Fig. 12 - Wavelet spectrum of the tangential velocity component.

These signals show high intermittency, as can be seen in Fig. 13, representing a small part of the entire interval of the acquisition, and reveal the presence of events (burst) that, if observed in the wavelet energy map (Fig.14), present maxima at frequencies typical of vortex wandering. However, these peaks which occur hieratically in time and at different frequencies reveal that this phenomenon is mostly intermittent and does not present any well defined periodic behavior in the center of the

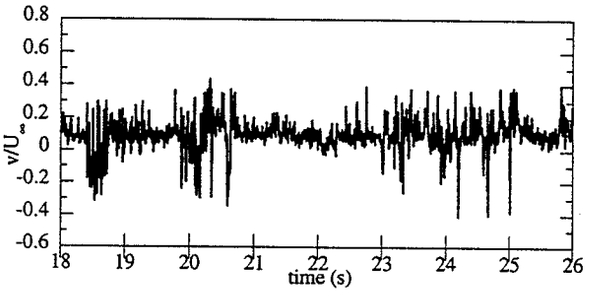

Fig. 13 - Example of the time history of the tangential velocity component at x/c=7 in the center of the mean vortex.

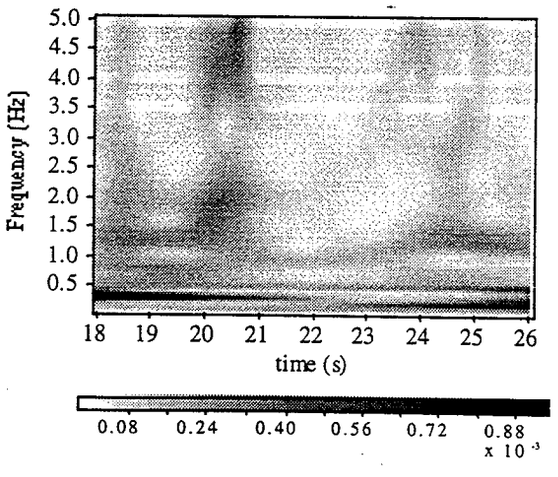

Fig. 14 - Energy wavelet map history of the tangential velocity component at x/c=7

LOMBARDI

mean vortex. Moving upstream, at x/c=1.0 the intermittent events are characterized by the same structure found at x/c=7.0, as can be seen from Fig. 15. This is confirmed by the behavior of the wavelet energy map shown in Fig. 16.

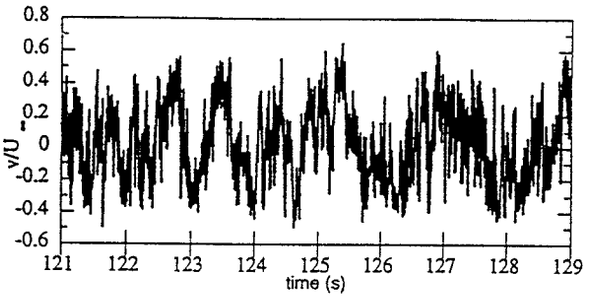

Fig. 15 - Example of the time history of the tangential velocity component at x/c=1 in the centre of the mean vortex.

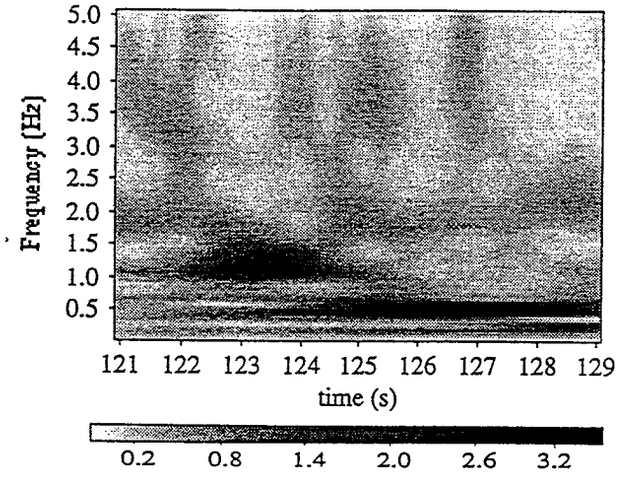

Fig. 16 - Energy wavelet map of the tangential velocity component at x/c=1 in the center of the mean vortex.

The origin of this unsteadiness is not well understood and may be triggered by some wind tunnel low frequency perturbations. In order to validate the accuracy of the statistical measurements a conditional average technique, based on the wavelet energy map, has been applied to the v-component of the time velocity signal. To this purpose a simple type of point average, i.e. the sampling signal is averaged only when a certain condition is satisfied, has been used. The conditioning function is provided by an X-wire probe kept fixed in the mean position of the vortex center while the sampling signal comes out from an other X-wire probe which traverses in the z-direction. First the wavelet energy map of the conditioning signal is evaluated obtaining the variation in time of the energy content corresponding to the different frequency scales. Then a frequency range f_{min}/f_{max} must be chosen considering typical frequencies of vortex wandering. If E(t) is the total energy amount at each time, fixing a threshold limit Tr, it is then possible to define an "intermittency" function H(t) defined as

$$H=1 \quad \text{if } E_m(t) > Tr\, E(t) \qquad (3)$$
$$H=0 \quad \text{elsewhere}$$

where E_m is the amount of energy contained in the range between f_{min} and f_{max}. Finally the conditioned statistical analysis is performed by averaging the sampling signal in the following way:

$$\langle f \rangle = \sum_{i=1}^{N} Hf \Big/ \sum_{i=1}^{N} H \qquad (4)$$

where N is the total number of samples. Different values of the threshold have been chosen; this technique is based on the hypothesis that the conditioning signal shows a larger energy contain (at the frequencies characteristic of the phenomenon) when the probe is interested by the presence of the vortex.

Fig. 17 shows the tangential velocity profile of the tip vortex for different values of the threshold Tr, averaging values larger than the threshold limit.

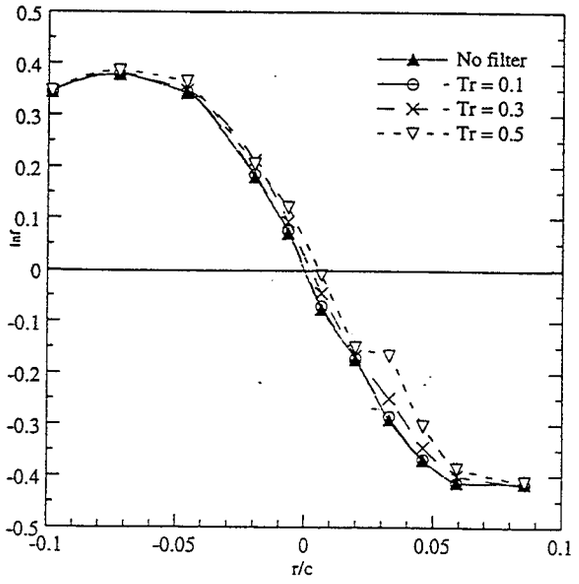

Fig. 17 - tangential velocity profile of the tip vortex for different values of the threshold; x/c=1.

From this figure it is not possible to depict the effect of the filtering even at high values of the filtering, i.e. when only a small percentage of the total amount of the samples are retained, showing that dimension and position of the vortex are not sensibly influenced, at least in this position close to the trailing edge. The same conclusion may be drawn considering the behavior of the turbulent fluctuations inside the vortex. This fact is probably due to

the limited amplitude oscillations, which characterize the vortex wandering at this position close to the trailing edge.

Conclusions

Experiments have been performed on a vortex produced by the tip of a tapered NACA 0012 half wing. Measurements have been accomplished at one chord length from the wing tip trailing edge by means of a new hot-wire techniques which allow to avoid the difficulties connected with the use and calibration of triple-wire probes and permits the use of considerably smaller and less intrusive probes. The technique developed allows the three mean velocity components and the whole Reynolds stress tensor to be evaluated Preliminary results presented in this paper permits to estimate dimension and shape of the vortex, localizing the core where the transversal velocity becomes maximum and the position of the vortex-center. At one chord the vortex is already rolled-up in an axisymmetric structure and no spiraling of the wake is shown. A maximum of negative vorticity close to the border of the vortex has been detected which may be due to the formation of a secondary structure induced by the main vortex. The principal stresses of the Reynolds stress tensor show an anisotropy of the Reynolds stress tensor that decreases moving downstream. In contrast with other results, presented in the literature, the maximum of the mean turbulent kinetic energy is located close to the vortex center. The results obtained by analyzing the signals with procedures based on the wavelet transform show the presence of the vortex wandering. However the effects of these low frequency unsteadiness in the statistical quantities seem to be significant only far downstream (5-7 chord length from the tip trailing edge).

Acknowledgments

The present investigation was financially supported by the Italian Ministry of University and Scientifical and Technological Research. We gratefully acknowledge G. Segneri, M. Cervo and N. Porciani.

References

[1] Lombardi, G. and Cannizzo, F., "High Aspect Ratio Wings: Tip Vortex Structure and its Numerical Implications," AIAA Paper 96-1961, (1996).

[2] Betz, A., "Behavior of Vortex System," NACA TM. 713, 1933.

[3] Lamb, H., "Hydrodynamics," 6th Edition, pag. 592, New York, Dover, 1945.

[4] Rossow, V. J., "On the Inviscid Rolled-Up Structure of Lift-Generated Vorticies," *Journal of Aircraft*, 10, No. 11, (1973), 647-650.

[5] Hoffman, E. R. and Joubert, P. N., "Turbulent Line Vortices," *Journal of Fluid Mech.*, 16, Pt. 3, (1963), 395-411.

[6] Batchelor, G. K., "Axial Flow in Trailing Line Vorticies," *Journal of Fluid Mech.*, 20, Pt. 4, (1964), 648-658.

[7] Moore, D. V. and Saffman, P. G., "Axial Flow in Laminar Trailing Vortices," *Proceedings of the Royal Society of London*, Series A, 333, (1973), 491-508.

[8] Staufenbiel, R. W., "Structure of Lift-Generated Rolled-Up Vortices," *Journal of Aircraft*, 21, No. 10, (1984), 737-744.

[9] Phillips, W. R. C., "The Turbulent Trailing Vortex During Roll-up," *Journal of Fluid Mech*, 105, (1981), 451-467.

[10] Hoeijmakers, H. W. M., "Computational Vortex Flow Aerodynamics," AGARD CP 342, Paper 18, (1983).

[11] Chigier, N. A. and Corsiglia V. R., "Tip vortices - velocity distributions," NASA TM-62087, (1971).

[12] Orloff , K. L., "Experimental investigation of upstream influence in a rotating flowfield," Ph.D. Thesis, University of California Santa Barbara, (1971).

[13] Accardo, L., Cenedese, A. and Cioffi, F., "Experimental analysis of tip vortex by laser Doppler Anemometry," *2nd Int. Symp. on Applications of Laser Anemometry to Fluid Mechanics*, Lisbon July 2-5, (1984).

[14] Green, S. I. and Acosta, A. J., "Unsteady Flow in Trailing Vorticies," *Journal of Fluid Mech.*, 227, (1991), 107-134.

[15] Shekarriz, A., Fu, T. C., Katzn J. and Huang, T. T., "Near-field behaviour of a tip vortex," AIAA J., 31, 112-118, (1993).

[16] Ramaprian, B.R. and Zheng Youxin, "Measurements in Rollup Region of the Tip Vortex from a rectangular Wing," *AIAA Journal*, 35, no. 12, (1997), 1837-1843.

[17] Devemport, W. J., Rife M. C., Liapis S. I. and Follin, G. J., "The structure and development of a wing tip vortex," *J. Fluid Mech.*, 227, 107-134, (1996).

[18] Cervo, M. and Porciani, N., "Sviluppo e messa a punto di un vorticimetro per lo studio di flussi non stazionari," (Setup and Development of a Vorticimeter for the Characterization of Unsteady Flows), Thesis, Department of Aerospace Engineering of Pisa, (1998).

[19] Buresti, G. and Talamelli, A, "On the error sensitivity of calibration procedures for normal hot-wire probes," *Meas. Sci. and Technol. 3*, 17-26, . (1992).

[20] Buresti, G. and Talamelli, A., "Hot wire measurement procedures for slanted and X probes in highly turbulent flows," ADIA 92-6, (1992).

[21] Jorgensen, F. E,. "Directional sensitivity of wire and fiber-film probes," DISA informations, 11, 31-37, (1971).

[22] Buresti, G., Fedeli, R., Lombardi G. and Marchetti, A., "Valutazione Sperimentale dei Carichi Aerodinamici su Ali in presenza di Superfici Portanti," ADIA 89-2, (1989).

[23] Cutler, A. D. and Bradshaw, P., "A crossed hot-wire technique for complex turbulent flows" Experiments in fluids, 12, 17-22, (1991).

[24] Chow, J. S., Zilliac, G. G. and Bradshaw, P., "Measurements in the Near-Field of a Turbulent Wing tip Vortex," AIAA Paper 93-0551, (1993).

[25] Segneri, G., "Indagine Sperimentale del Campo di Velocita' a Valle di sistemi Portanti," (Experimental Investigation on the Flow Field downstream Lifting Surfaces), Thesis, Department of Aerospace Engineering of Pisa, (1997).

[26] Farge, M., Kevlahan, N., Perrier, V. and Goirand, E., "Wavelet and Turbulence," Proc. of IEEE, 84, 639-699, (1996).

[27] Buresti, G., Lombardi, G. and Talamelli, A, "Low Aspect-Ratio Triangular Prisms in Cross-Flow: Measurements of the Wake Fluctuating Velocity Field," Proc. of 2nd European and African Conference on Wind Enginnering, Genova, (1997).